Journal of Innovative Optical Health Sciences
Vol. 3, No. 1 (2010) 61–67

World Scientific
www.worldscientific.com

DETECTING CEREBRAL ARTERIES AND VEINS: FROM LARGE TO SMALL

PENG MIAO*,†, MINHENG LI*, NAN LI†, ABHISHEK REGE†,
YISHENG ZHU*, NITISH THAKOR† and SHANBAO TONG‡,§
*Department of Biomedical Engineering, Shanghai Jiao Tong University
Shanghai 200240, China
†Department of Biomedical Engineering, Johns Hopkins University
Baltimore, MD 21205, USA
‡Med-X Research Institute, Shanghai Jiao Tong University
Shanghai 200230, China
§shanbao.tong@gmail.com

In this paper, a model-based reconstruction technique is proposed to simultaneously measure the relative deoxyhemoglobin concentration and the relative blood flow velocity in cerebral cortex. With the help of this model-based reconstruction technique, artifacts due to nonuniform laser illumination and curvature of cortex are efficiently corrected. The results of relative deoxyhemoglobin concentration and relative blood flow velocity are then used to detect and distinguish cerebral arteries and veins. In an experimental study on rat, cerebral blood vessels are segmented from the reconstructed blood flow image by Otsu multiple threshold method. Afterwards, arteries and veins are distinguished by a simple fuzzy criterion based on the information of relative deoxyhemoglobin concentration.

Keywords: Intraoperative detection; optical intrinsic signal (OIS); laser speckle imaging (LSI); laser speckle contrast analysis (LASCA); model based reconstruction.

1. Introduction

Detecting cerebral arteries and veins is very important for studying cerebral blood supply and cortical vasculature network.[1] Furthermore, it will be very helpful to provide an intraoperative distinction of cerebral arteries and veins during brain surgery.[2] Compared with other techniques (like CT, MRI, and PET), optical imaging method offers specific advantages including easy implementation, high spatial and temporal resolution, relatively noninvasiveness, and the relevance to underlying functional changes.[3] Among the variety of optical imaging methods, two methods, optical intrinsic signal (OIS)[4] imaging and laser speckle imaging (LSI),[5] offer the advantage of obtaining functional information about brain oxygenation and blood flow. They are the focus of this study.

OIS imaging is based on the light absorption properties of cortical tissue. When imaging with light of 600–635 nm, the oxyhemoglobin absorption is negligible compared with that of deoxyhemoglobin. Therefore area with higher level of deoxyhemoglobin concentration C (e.g. the veins) leads to more absorption and thus makes the corresponding area darker, i.e. smaller intensity values, in the image. Ideally, the relation for the relative concentration of deoxyhemoglobin in artery, tissue, and vein satisfies: $C_{\text{artery}} < C_{\text{tissue}} < C_{\text{vein}}$.[6] As a

‡Corresponding author.

two-dimensional optical imaging technique with high spatial and temporal resolution, LSI has been used to study the cerebral blood flow and blood vasculature based on the scattering property of blood cells. Using laser speckle contrast analysis (LASCA),[7,8] the contrast value K^2 (the squared ratio of temporal standard derivation σ_t of the intensity to the mean intensity $\langle I \rangle$) of any pixel in the image is related to the velocity v (Eq. (1)).

$$K^2 = \left(\frac{\sigma_t}{\langle I \rangle}\right)^2 \propto \frac{1}{v}. \tag{1}$$

The relations for blood flow velocity in artery, tissue, and vein satisfy $v_{\text{artery}} > v_{\text{tissue}}$ and $v_{\text{vein}} > v_{\text{tissue}}$.[6] Combining the information of deoxyhemoglobin concentration and blood flow velocity, the arteries and veins can therefore be distinguished.

In this paper, the inhomogeneous model for nonuniform laser illumination and the curvature of imaging cortex is estimated to reconstruct the images of relative deoxyhemoglobin concentration and relative blood flow velocity simultaneously. Because the scattering interferences produced by laser illumination leads to noisy fluctuations in the reconstructed image of relative deoxyhemoglobin concentration, a simple fuzzy criterion is used to distinguish arteries and veins. In an experimental study, rat's cerebral arteries and veins are distinguished using this new technique.

2. Method

2.1. *Optical imaging system*

A coherent 635 nm He–Ne laser beam source (1805P, Uniphase, CA) is used to illuminate the cortex obliquely with a 30° angle of incidence. The laser beam was reshaped by a lens to expand illuminating range. A 12-bit cooled CCD camera (Sensicam SVGA, Cooke, MI) with a 60 mm macro (1:1 maximum reproduction ratio) f/2.8 lens was held by a rack and focused on the imaging area. The image resolution is 704 by 704 pixels corresponding to an area of 4.7 by 4.7 mm^2. The exposure time was set to 2 ms and the frame rate was 11 fps. The imaging system is shown in Fig. 1.

Suppose the illumination is uniform and the surface of imaging cortex is flat, then the relative deoxyhemoglobin concentration and the relative blood flow velocity can be obtained simultaneously as follows: (1) the averaged intensity of each pixel across sequentially recorded images is calculated to obtain the relative deoxyhemoglobin concentration map, which may still be contaminated by the scattering interferences; (2) the contrast value K^2 is used to estimate the relative blood flow velocity (Eq. (1)).

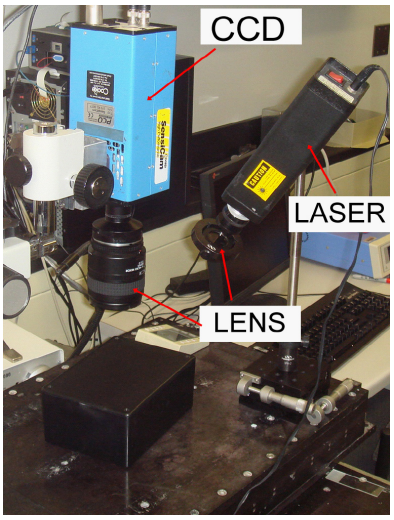

Fig. 1. The optical imaging system.

2.2. *Model based reconstruction*

In practice, nonuniform laser illumination and the curvature of cortex result in significant inhomogeneous impact and bias in the estimations of both deoxyhemoglobin concentration and cerebral blood flow,[9] which thus makes the detection of arteries and veins unreliable. To solve this problem, we need to correct the OIS image I_{OIS} and LSI image I_{LSI} from the biased OIS image $\tilde{I}_{\text{OIS}}$ and biased LSI image $\tilde{I}_{\text{LSI}}$, respectively, before the detection of arteries and veins. In this study, the inhomogeneous impact, modeled as joint effect from nonuniform illumination and cortex curvature, is estimated by 1D curve fitting technique, which is then used to reconstruct the OIS and LSI images.

When a laser light illuminates the surface obliquely, the effect of elliptic beam illumination can be modeled as a 2D Gaussian function (Eq. (2)).

$$M_1(x,y) = a \exp\left(-\left(\left(\frac{x-b_1}{r_1}\right)^2 + \left(\frac{y-b_2}{r_2}\right)^2\right)\right), \tag{2}$$

where (x, y) is the Cartesian coordinates of illumination area, a is the scale coefficient, (b_1, b_2) is the center of Gaussian function, and r_1 and r_2 are the semi-axis length along x-axis and y-axis, respectively.

While the influence of cortex curvature can be approximately modeled as a part of elliptic paraboloid (Eq. (3)).

$$M_2(x,y) = d\left(\frac{(x-p_1)^2}{q_1^2} + \frac{(y-p_2)^2}{q_2^2}\right), \quad (3)$$

where d is the scale coefficient, (p_1, p_2) is the center of elliptic paraboloid, and q_1 and q_2 are the semi-axis length along x-axis and y-axis, respectively.

Since the effects of Gaussian laser illumination and cortex curvature are multiplicative, the model for total inhomogeneous impact is modeled as follows (Eq. (4)):

$$M(x,y) = M_1(x,y) \cdot M_2(x,y). \quad (4)$$

The biased OIS image $\tilde{I}_{\mathrm{OIS}}$ can be described as Eq. (5).

$$\tilde{I}_{\mathrm{OIS}}(x,y) = M(x,y) \cdot I_{\mathrm{OIS}}(x,y). \quad (5)$$

To reconstruct the unbiased $I_{\mathrm{OIS}}(x,y)$, we are going to estimate the inhomogeneity model $M(x,y)$ from the biased OIS image $\tilde{I}_{\mathrm{OIS}}(x,y)$. However, it is practically impossible to fit the 2D model $M(x,y)$ based on $\tilde{I}_{\mathrm{OIS}}(x,y)$. Furthermore, the effect of cortex curvature is always more complicated than a simple elliptic paraboloid. Therefore, to estimate $M(x,y)$ at low computing cost, 1D curve fitting technique is used along each diameter of the ellipse. Based on Eq. (5), the intensity values along each diameter are derived as follows:

$$\tilde{I}_{\mathrm{OIS}}(l) = M(l) \cdot I_{\mathrm{OIS}}(l), \quad (6)$$

where l is the coordinate along the diameter (the center point as the origin).

The 1D model $M(l)$ (Eq. (7)) is derived from the 2D model $M(x,y)$ (Eq. (3)). Correspondingly, the effect of Gaussian illumination is represented as a 1D Gaussian function: $M_1(l) = s(l^2 + cl + t)$. While the effect of cortex curvature is modeled as a quadratic function: $M_2(l) = \exp(-(l/r)^2)$. Therefore, Eq. (4) can be written as:

$$M(l) = M_1(l) \cdot M_2(l), \quad (7)$$

where l is the coordinate along the diameter (the center point as the origin), (s, c, t) are parameters of the quadratic function, and r is the shape parameter of the Gaussian function.

In Eq. (6), if $I_{\mathrm{OIS}}(l)$ is approximately a constant, then $M(l)$ can be easily estimated by 1D curve fitting technique. Since the OIS image is related to the deoxyhemoglobin concentration, there is large intensity decay in veins, which makes the direct curve fitting inaccurate. To eliminate the intensity decay and other noises, a median–mean filtering process with adaptive window is performed before the curve fitting. The data along each diameter $\tilde{I}_{\mathrm{OIS}}(l)$ is smoothened first by the median filter with a window size $2R$ and then by the mean filter with a window size $R(R = 1/20$ of image size).

The smoothened data is then used to estimate the model $M(l)$. Each parameter in the 1D model (Eq. (7)) is estimated by curve fitting technique[10] using nonlinear least square method. Finally, the 2D model $M(x,y)$ is constructed. The reconstructed OIS image I_{OIS} and LSI image I_{LSI} are calculated as below:

$$I_{\mathrm{OIS}}(x,y) = \frac{\tilde{I}_{\mathrm{OIS}}(x,y)}{M(x,y)}, \quad (8)$$

$$I_{\mathrm{LSI}}(x,y) = \frac{\tilde{I}_{\mathrm{LSI}}(x,y)}{M(x,y)}. \quad (9)$$

2.3. *Detecting and distinguishing arteries and veins*

Using the relative blood flow information in the reconstructed LSI image I_{LSI}, the blood vessels are automatically segmented by the Otsu multiple threshold method.[11] Ideally the relation for deoxyhemoglobin concentration C in artery, tissue, and vein is $C_{\mathrm{artery}} < C_{\mathrm{tissue}} < C_{\mathrm{vein}}$, so the intensity value of artery in the reconstructed OIS image is greater than that of tissue, and the intensity value of vein is less than that of tissue. In practice, laser always produces the noisy interferences in the reconstructed OIS image, which makes it difficult to distinguish arteries and veins.

In this study, we propose a simple fuzzy criterion method to distinguish arteries and veins utilizing the noisy information in the reconstructed OIS image. From the vessel segmentation image, the largest artery and vein are identified manually based on the anatomical features. Using the noisy absorption information in the reconstructed OIS image, a percentage P_{artery} is calculated for the largest artery that more than P_{artery} of pixels in the largest artery have intensity greater than the average intensity ($\bar{I}_{\mathrm{tissue}}$) in tissue area. Similarly a percentage P_{vein} is defined for the largest vein. Then a simple fuzzy criterion, e.g. the vessel containing more than P_{artery} of points with intensity larger than $\bar{I}_{\mathrm{tissue}}$ is artery and the vessel containing more than P_{vein} of points with intensity smaller

than $\bar{I}_{\text{tissue}}$ is vein, is constructed to distinguish other arteries and veins.

3. Experiment

3.1. *Animal preparation*

The animal experiment protocol in this study has been approved by the Animal Care and Use Committee of the Johns Hopkins Medical Institutions. The female Sprague–Dawley rats (~ 300 g) were anesthetized with intraperitoneal (IP) injection of sodium pentobarbital (50 mg/kg). The rats were constrained in a stereotaxic frame (model 975, Kopf Instruments, Tujunga, CA) after unconsciousness. A midline incision was made over the scalp and the tissues over the bones were cleaned with a blade. A 10 by 10 mm cranial window overlying the center of right somatosensory cortex (centered of 5.5 mm lateral and 2.5–3.0 mm caudal from the bregma) was thinned with a high-speed dental drill (Fine Science Tools Inc. North Vancouver, Canada) equipped with 1.4 mm steel burr until half transparent.

3.2. *Imaging protocol*

The cranial window is imaged by the imaging system described earlier (Fig. 1). 80 raw images were

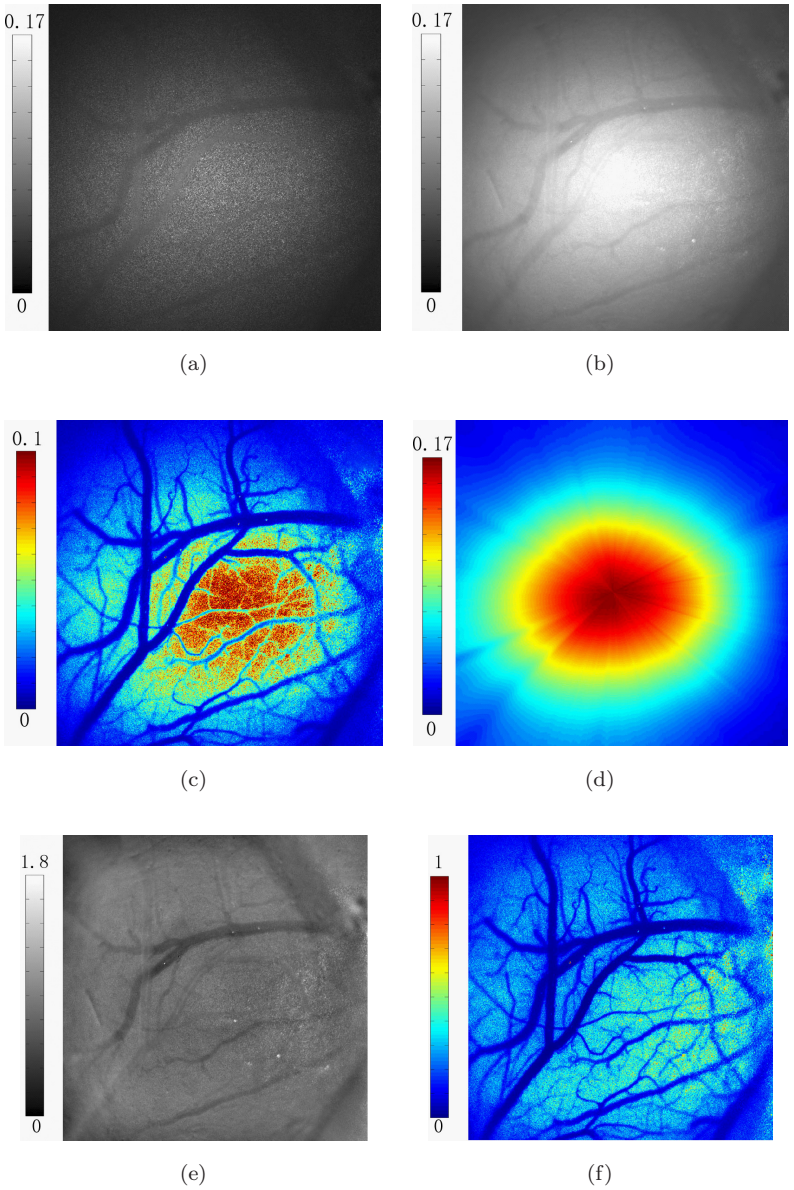

Fig. 2. Model-based reconstruction results: (a) one of the raw images; (b) the biased OIS image; (c) the biased LSI image; (d) the estimated inhomogeneous impact model; (e) the reconstructed OIS image; and (f) the reconstructed LSI image.

recorded by the CCD camera in the experiment. Using the model-based reconstruction in Sec. 2, the reconstructed results I_{OIS} and I_{LSI} were obtained to detect and distinguish arteries and veins.

4. Results

4.1. *Reconstruction of OIS and LSI images*

Figure 2(a) shows one frame recorded by the CCD camera during the experiment. Figures 2(b) and 2(c) show the biased OIS image $\tilde{I}_{\mathrm{OIS}}$ and LSI image $\tilde{I}_{\mathrm{LSI}}$, respectively. Clearly, in both Figs. 2(b) and 2(c), the inhomogeneity makes the measurement of relative deoxyhemoglobin concentration and relative blood flow velocity biased. The inhomogeneity model $M(x, y)$ is estimated and shown in Fig. 2(d). Figures 2(e) and 2(f) show the reconstructed OIS image I_{OIS} and LSI image I_{LSI} after the model-based reconstruction, in which the inhomogeneous impact is effectively eliminated.

4.2. *Detecting and distinguishing cerebral arteries and veins*

After the reconstruction, blood vessels are automatically segmented from the LSI image using the Otsu multiple threshold method. Then, six vessels (V1–V6) are selected manually for the following discussions (Fig. 3(c)). V1 and V2 are two largest vessels in the imaging area. Based on the anatomical feature of rat's cerebral vasculature network, V1 is an artery and V2 is a vein.

For each pixel (x, y) in the vessel area, we construct a two-dimensional vector $(I_{\mathrm{OIS}}(x, y), I_{\mathrm{LSI}}(x, y))$ which contains the information of both relative deoxyhemoglobin concentration and relative blood flow velocity. The vector $(I_{\mathrm{OIS}}(x, y), I_{\mathrm{LSI}}(x, y))$ of every pixel in V1 (red circles) and V2 (blue circles) is plotted in Fig. 3(d) where x-axis stands for $I_{\mathrm{OIS}}(x, y)$ and y-axis stands for $I_{\mathrm{LSI}}(x, y)$. Because of the noisy interferences produced by laser illumination, the pixels' $I_{\mathrm{OIS}}(x, y)$ in either vessel are spreading out over a comparably large range. Although there are overlaps between V1 and V2, the cluster of red circles (V1) is quite different from that of the blue circles (V2). Based on the noisy information in OIS image, more than 70% (P_{artery}) of points in V1 are with $I_{\mathrm{OIS}}(x, y)$ larger than 0.9 ($\bar{I}_{\mathrm{tissue}}$), while greater than 70% (P_{vein}) of points in V2 are with $I_{\mathrm{OIS}}(x, y)$ less than 0.9.

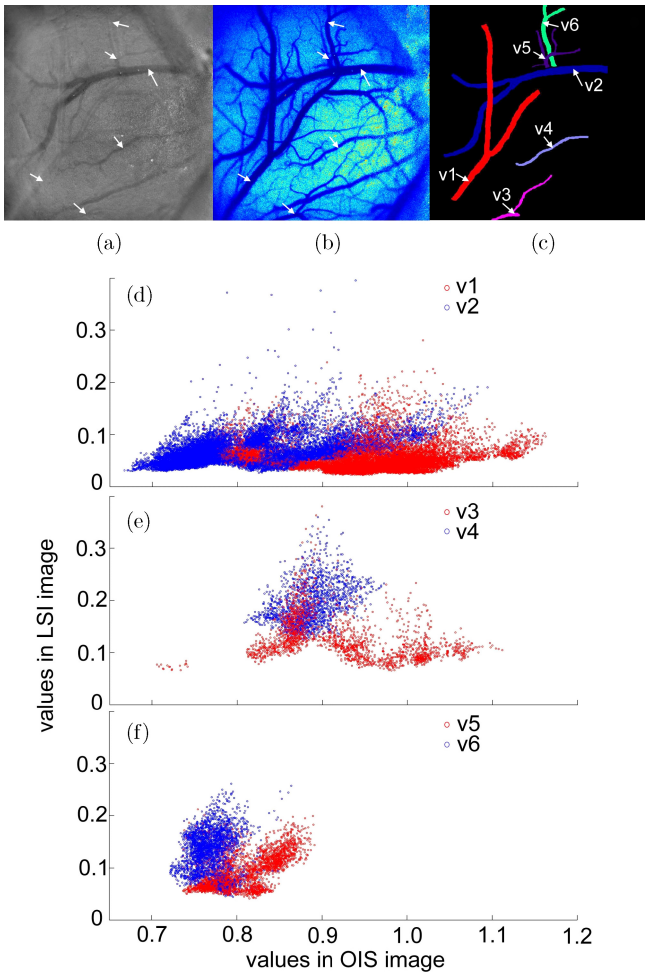

Fig. 3. The detection of arteries and veins: (a) and (b) are the reconstructed OIS and LSI images, respectively; (c) shows the six selected vessels (V1–V6) for analysis; (d), (e), and (f) plot the values in OIS and LSI images for each point in the vessels, (d) is for V1 and V2, (e) is for V3 and V4, and (f) is for V5 and V6.

A simple criterion is thus constructed to distinguish rat's cerebral arteries and veins: a vessel containing more than 70% of points with $I_{\mathrm{OIS}}(x, y)$ greater than 0.9 is an artery, otherwise it is a vein. Using this criterion, V3 is a small artery while V4 is a small vein (Fig. 3(e)). In Fig. 3(f), both V5 and V6 are small veins; this conclusion can also be verified by the fact that V5 and V6 are two branches of the larger vein V2. The vessel types of V3–V6 were confirmed independently by an experienced clinician.

5. Discussion

The nonuniform model of laser illumination can be alternatively estimated using the reflectance image of an ideal, smooth surface. However, the subject-dependent inhomogeneous impact of cortex

curvature is really difficult to measure by other ways, for example, 3D methods like magnetic resonance imaging would be inordinately expensive and difficult to implement. The proposed model-based reconstruction is totally an optical method and relies only on post-processing that needs no extra hardware or experiment.

In this study, rat's cerebral arteries and veins are segmented from the reconstructed LSI image using Otsu multiple threshold method which usually needs about 12 s to process a 704 by 704 image. In practice, with the help of human vision system, a human observer can easily and quickly distinguish the blood vessels. The model based reconstruction technique shows the potential to be an intraoperative monitoring technique in brain surgery. Actually surgeons may easily distinguish arteries and veins just looking at both the reconstructed OIS and LSI images using their experiences.

However, when automation is required, our approach will be useful. Such automation may be needed in imaging brain pathology such as due to tumor.[12] Another application area is a minimally invasive surgery.[13] In such situations, automatic differentiation of artery or vein by optical method will be useful. Other application areas include physiological studies of cerebral blood flow, where perturbations that mimic injury or insult, such as hypoxia or ischemia, alter flow in the brain vasculature.[14] Knowing the arterial and venous structures and the flow within these vessels would be useful in quantifying effects of stroke or drugs for stroke therapy.[15]

6. Conclusion

In this paper, we proposed a model-based technique to reconstruct the OIS and the LSI images simultaneously. After the segmentation of blood vessels from the reconstructed LSI image, cerebral arteries and veins can be distinguished using a fuzzy criterion applied to the noisy deoxyhemoglobin information in the reconstructed OIS image. In the experimental study, rat's cerebral blood arteries and veins were detected and distinguished using the new method. This new technique is useful for pathological and physiological studies of cerebral blood flow and metabolism.

Acknowledgments

This work is supported by NIH/NIA1R01AG 029681. S. Tong is also supported by the New Century Talent Program by the Ministry of Education of China, and Shanghai Shuguang Program (07SG13). P. Miao is also supported by the China Scholarship Council.

References

1. S. Strandgaard, J. Olesen, E. Skinhoj, N. A. Lassen, "Autoregulation of brain circulation in severe arterial hypertension," *Br. Med. J.* **1**, 507–510 (1973).
2. L. D. Lunsford, D. Kondziolka, D. J. Bissonette, "Intraoperative imaging of the brain," *Stereotact. Funct. Neurosurg.* **66**, 58–64 (1996).
3. K. Sato *et al.*, "Intraoperative intrinsic optical imaging of neuronal activity from subdivisions of the human primary somatosensory cortex," *Cereb. Cortex* **12**, 269–280 (2002).
4. A. Grinvald, E. Lieke, R. D. Frostig, C. D. Gilbert, T. N. Wiesel, "Functional architecture of cortex revealed by optical imaging of intrinsic signals," *Nature* **324**, 361–364 (1986).
5. A. K. Dunn, H. Bolay, M. A. Moskowitz, D. A. Boas, "Dynamic imaging of cerebral blood flow using laser speckle," *J. Cereb. Blood Flow Metab.* **21**, 195–201 (2001).
6. L. Edvinsson, E. T. MacKenzie, McCulloch, *Cerebral Blood Flow and Metabolism*, Raven Press, New York (1993).
7. J. D. Briers, S. Webster, "Laser speckle contrast analysis (LASCA): A nonscanning, full-field technique for monitoring capillary blood flow," *J. Biomed. Opt.* **1**, 174–179 (1996).
8. H. Cheng, Q. Luo, S. Zeng, S. Chen, J. Cen, H. Gong, "Modified laser speckle imaging method with improved spatial resolution," *J. Biomed. Opt.* **8**(3), 559–564 (2003).
9. P. Miao, N. Li, A. Rege, S. Tong, N. Thakor, "Model based reconstruction for simultaneously imaging cerebral blood flow and deoxyhemoglobin distribution," in *31th Annual International Conference of the IEEE Engineering in Medicine and Biology Society (EMBS)*, IEEE, Minneapolis, MN (2009).
10. H. Motulsky, A. Christopoulos, *Fitting Models to Biological Data Using Linear and Nonlinear Regression: A Practical Guide to Curve Fitting*, Oxford University Press, USA (2004).
11. N. Otsu, "A threshold selection method from gray-level histograms," *IEEE Trans. SMC* **9**, 62–69 (1979).
12. J. Holash, P. C. Maisonpierre, D. Compton, P. Boland, C. R. Alexander, D. Zagzag, G. D. Yancopoulos, S. J. Wiegand, "Vessel cooption, regression, and growth in tumors mediated by angiopoietins and VEGF," *Science* **284**(5422), 1994–1998 (1999).

13. M. J. Mack, "Minimally invasive and robotic surgery," *JAMA* **285**(5), 568–572 (2001).
14. D. W. Choi, "Cerebral hypoxia: Some new approaches and unanswered questions," *J. Neurosci.* **10**(8), 2493–2501 (1990).
15. A. G. Sorensen, W. A. Copen, L. Østergaard, F. S. Buonanno, R. G. Gonzalez, G. Rordorf, B. R. Rosen, L. H. Schwamm, R. M. Weisskoff, W. J. Koroshetz, "Hyperacute stroke: simultaneous measurement of relative cerebral blood volume, relative cerebral blood flow, and mean tissue transit time," *Radiology* **210**(2), 519–527 (1999).